

# Comparative Performance of DVR and STATCOM for Voltage Regulation in Radial Microgrid with High Penetration of RES

Case Study

## Ritika Gour

Delhi Technological University,  
Electrical Engineering Department, Delhi, India  
riti113@gmail.com

## Vishal Verma

Delhi Technological University,  
Electrical Engineering Department, Delhi, India

**Abstract** – In recent years, the penetration of renewable energy sources (RES) in microgrids and distribution system feeders has increased manifold. Moreover, the advancement of power electronics-based devices in the distribution system has significantly increased the number of sensitive loads. Variations in the voltage under intermittent RES create functional problems with sensitive loads, necessitating voltage regulators (VR) installation. In this paper, two custom power devices: dynamic voltage restorer (DVR) and static synchronous compensator (STATCOM), used for voltage regulation in a microgrid, are investigated under different operating conditions. The efficacy of DVR and STATCOM for voltage regulation in an 11-node radial microgrid with high penetration of RES is simulated under a MATLAB Simulink environment. Furthermore, the simulated microgrid voltage profile results are analyzed to evaluate the efficacy of both voltage regulators.

---

**Keywords:** RES, intermittency, CPL, microgrid, voltage regulation, DVR, STATCOM

---

## 1. INTRODUCTION

A microgrid is a local energy grid with a group of connected energy sources and loads that usually operate in synchronization with the conventional grid but can also operate independently in the event of any anomaly. Various renewable energy sources (RES) can be connected to the microgrid such as solar panels, wind turbines, etc. With the advancement of technology, the diminishing supply of conventional power sources and many environmental and socio-economic factors have raised RES penetration in the microgrid [1-4]. Increased renewable energy in the microgrid provides numerous benefits, like increased local power availability, low-cost, clean energy, increased reliability and resilience, reduced grid congestion and peak loads, etc. However, the intermittent nature of RES creates power fluctuations and large variations in the voltage profile. As a result of the unpredictable nature of these RES, the microgrid operator is unable to schedule the load, posing a risk to the entire system. Furthermore, the widespread use of power electronics-based devices in residential and commercial loads has significantly increased the number of sensitive loads. Power and voltage variations due to high penetration of RES may result in the maloperation of these sensi-

tive loads, damage to equipment, and cascading faults. These challenges deteriorate the power quality of the microgrids which causes instability and monetary losses for both the microgrid and the consumer. [5].

The variability of demands and intermittency of renewable sources necessitates the methods to deal with variation in the voltage of the microgrid. Mitigation of the negative effects of intermittent RES is achieved by adopting different methods for regulating the voltage of the microgrid. The static synchronous compensator (STATCOM) and the dynamic voltage restorer (DVR) are two custom power devices that are generally installed in the distribution system to regulate voltage profile [8-10]. DVR regulates the voltage at the point of common coupling (PCC) by supplying/absorbing the voltage in series with the PCC voltage and is connected to the feeder through an injection transformer [5] [9-12]. On the other hand, STATCOM is connected in shunt with the feeder, thereby allowing the supply or absorption of current from the feeder, with an effect on the voltage as well [10] [13].

The efficacy of DVR and STATCOM for voltage regulation in microgrids with significant RES penetration is in-

vestigated in this paper by simulating an 11-node grid-connected radial microgrid in the MATLAB/Simulink environment. Findings of the simulation are then used to draw a microgrid voltage profile from the grid mains to the last node in the presence of the STATCOM and DVR, one by one, and their efficacy is assessed.

Section 2 describes the block diagram of the considered system, and Section 3 discusses the block diagram and phasor diagram of both voltage regulators DVR and STATCOM. Further Section 4 includes MATLAB Simulink and performance evaluations of both STATCOM and DVR.

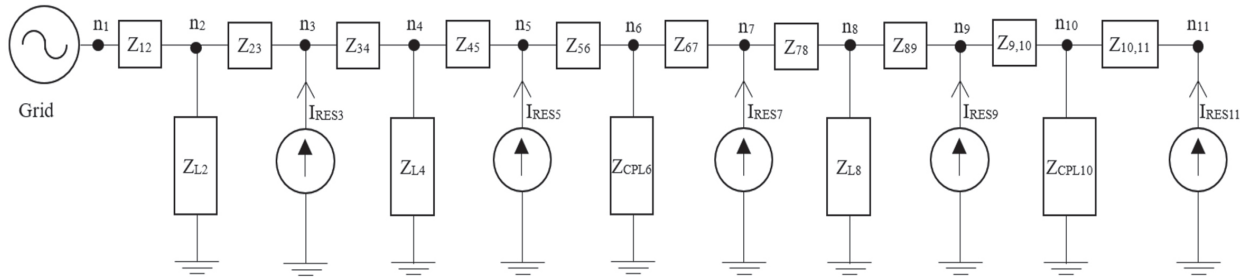


**Fig. 1.** Single line diagram of system under consideration

## 2. SYSTEM CONFIGURATION

The system under consideration is shown in Fig. 1. Considered a system an 11-node grid connected radial microgrid. The voltage source/grid is assumed to be a reference node ( $n_1$ ). RES sources ( $I_{RES_i}$ ) and loads  $Z_{L_i}$  are connected alternatively throughout the radial microgrid (where 'i' is the node number with respect to the reference node). All the RESs are connected on odd nodes ( $n_3, n_5, n_7, n_9$  and  $n_{11}$ ) and all the loads are connected on even nodes ( $n_2, n_4, n_6, n_8$  and  $n_{10}$ ) with respect to the reference node ( $n_0$ ). In the considered system RESs are connected to the microgrid as a current source feeding the microgrid through a current-controlled voltage source converter (VSC). Loads connected to the microgrid are of two types: constant impedance load (CIL) and constant power load (CPL). CILs are connected at node 2, node 4, and node 8. Generalized expression for the impedance  $Z_{L_i}$  of the CIL is given as:

$$Z_{L_i} = \frac{(V_{n_i}(\text{rated}))^2}{P_{L_i} + jQ_{L_i}} \quad (1)$$

Where  $V_{n_i}(\text{rated})$  is rated voltage at the node and  $P_{L_i} + jQ_{L_i}$  is rated power of the load (power consumed by the load at rated voltage).

CPLs are connected at node 6 and node 10. The impedance of CPL is dynamic in nature, it shows a negative impedance characteristic, and power drawn ( $P_{CPL_i}$ ) remains constant irrespective of the instantaneous voltage ( $V_{n_i}$ ) at its terminal. CPL changes load current according to the voltage level so that it can draw a constant power from the microgrid. Generalized expression for the dynamic impedance of the CPL is given as [14-15]:

$$Z_{CPL_i} = \frac{(V_{n_i})^2}{P_{CPL_i}} \quad (2)$$

For ease of study, certain assumptions are made which are as follows:

- RES and loads are placed alternatively on the microgrid with uniform distancing.
- Microgrid is part of distribution feeder with R/X ratio  $\approx 8$  such that feeder impedance is  $0.642 + j0.0833 \Omega/\text{km}$  [16].
- Length of each section is 0.5 km.

## 3. OPERATING PRINCIPLE OF DVR AND STATCOM

### 3.1 OPERATING PRINCIPLE OF DVR

DVR is a custom power device connected in series with the feeder as seen in Fig. 2(a). DVR generally comprises of injection transformer, ripple filter, VSC and DC link. The DC voltage on the DC link is converted to AC by VSC as required for voltage regulation. A further ripple filter is used to filter the AC voltage generated from VSC before the injection transformer injects it into the line.

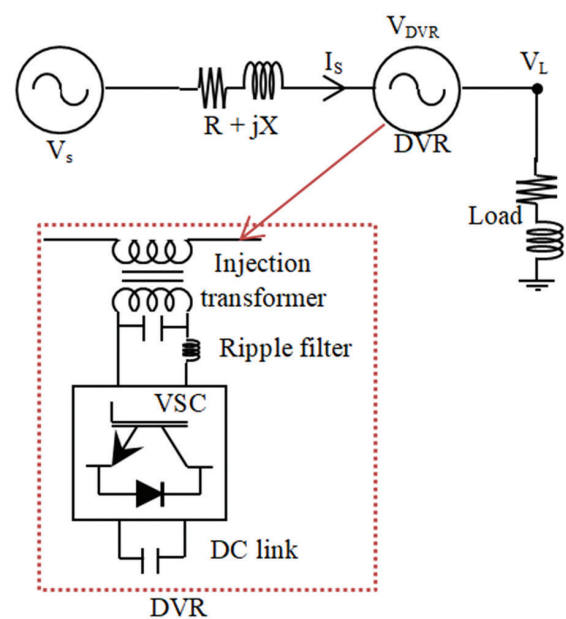


**Fig. 2.(a)** Block diagram for voltage regulation by DVR

The injection transformer is a low leakage impedance transformer that connects the DVR to the feeder in series. On the DC side of the VSC, a capacitor is typically present to maintain the DC link voltage. To increase the range of regulation of DVR, batteries can also be placed on the DC side. The phasor diagram for the DVR voltage regulation is shown in Fig. 2(b). From the phasor diagram, it can be observed that the net voltage at the terminal of DVR is equal to the phasor sum of the previous terminal voltage and DVR injected/absorbed voltage.

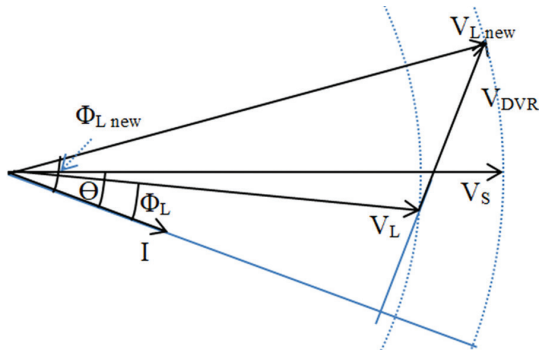


**Fig. 2.(b)** Phasor diagram of DVR for voltage regulation

Synchronous reference frame theory is used to control the gating pulses of VSC in DVR, which are subsequently used for controlling the injection of requisite voltage from the DVR [9]. Fig. 2(c) shows the block diagram of the control scheme.

The difference between the measured voltage, from the terminals of DVR, and the rated voltage is passed through the proportional-integral (PI) controller for generating the DVR reference (injection/absorption) voltage. Usually, the voltage regulation is done with the reactive component of voltage, which means that the DVR reference voltage is generally the quadrature-axis (q-axis) component ( $V_q$ ). Nevertheless, if the voltage required to regulate the terminal voltage exceeds the limit of the DVR's reactive capacity, then  $V_q$  is reduced with a simultaneous increase of  $V_d$  to regulate the terminal voltage of the DVR. Subsequently, reverse park transformation is performed on the reference  $V_d$  and  $V_q$  through dq to abc transformation. The gating pulses of VSC are generated by passing the resultant abc reference signal through the pulse width modulator (PWM) block. These gating pulses are further used to control the ON/OFF different switches of VSC, for requisite voltage injection, to regulate the voltage at the DVR terminal.

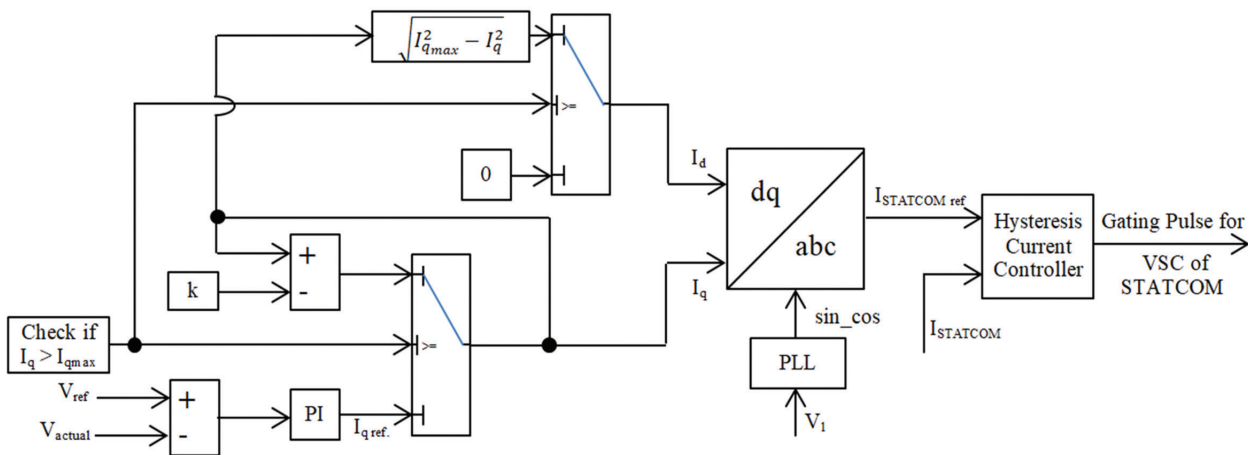


**Fig. 2. (c)** Block diagram of control of STATCOM

### 3.2 OPERATING PRINCIPLE OF STATCOM

Another custom power device investigated in the paper is STATCOM, which is in shunt with the feeder, as illustrated in Fig. 3(a). The VSC converts DC to AC, and after passing through the ripple filter, the output current from the VSC is sent to the microgrid. In the design shown in Fig. 3(a), it is connected in parallel to the load connected at nodes 6 and 10. Fig. 3(b) shows a phasor diagram for its voltage regulation.

The synchronous reference frame theory is also used to control the VSC of STATCOM. Fig. 3(c) depicts the control approach for generating the gating pulses for the VSC of STATCOM. The controller senses the volt-

age at its terminal, and then the difference between the sensed voltage and the reference voltage is passed through the PI controller, generating the q-axis component of the current ( $I_q$ ). As shown in the block diagram, when the STATCOM approaches its reactive power limit, the q-axis component is reduced, and the d-axis component ( $I_d$ ) is increased, as done in the case of DVR. To generate the reference STATCOM current ( $I_{STATCOMref}$ ), the reference values of  $I_d$  and  $I_q$  are transformed into reference abc signal through reverse PARKs transformation. Furthermore, the gating pulses for VSC switches are generated by passing STATCOM reference ( $I_{STATCOMref}$ ) current and actual ( $I_{STATCOM}$ ) current through a hysteresis current controller.

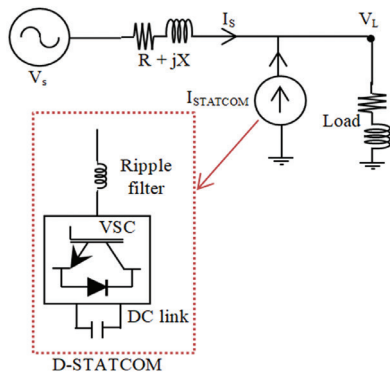


**Fig. 3.(a)** Block diagram for voltage regulation by STATCOM

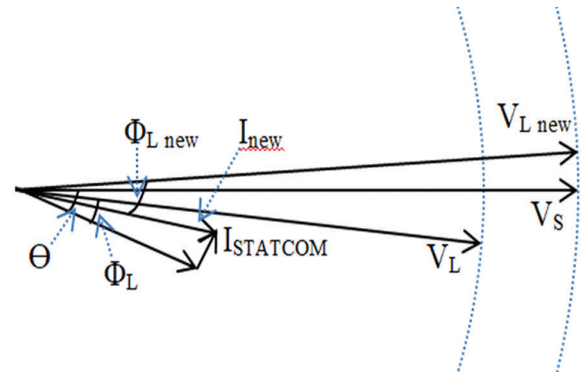


**Fig. 3.(b)** Phasor diagram of STATCOM for voltage regulation

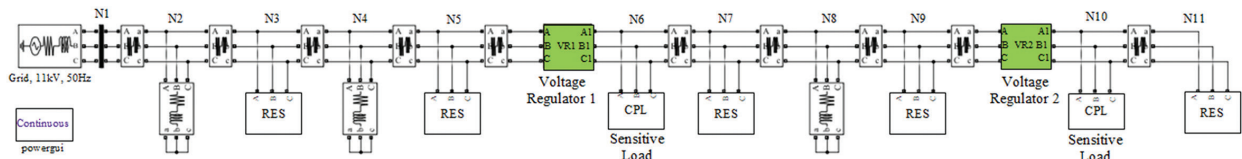


**Fig. 4.(a)** MATLAB/Simulink diagram for considered radial microgrid

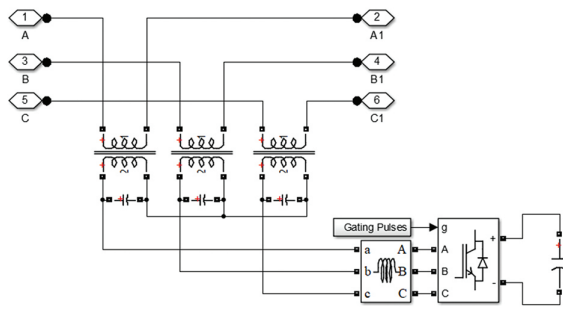


**Fig. 4.(b)** MATLAB/Simulink diagram for DVR

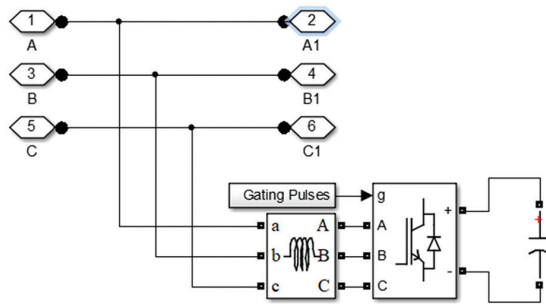


**Fig. 4.(c)** MATLAB/Simulink diagram for STATCOM

#### 4. PERFORMANCE EVALUATION OF DVR AND STATCOM

Simulations in the MATLAB/Simulink environment are done to investigate the efficacy of DVR and STATCOM in the considered 11 nodes radial microgrid. MATLAB simulation diagram of the microgrid with RES and voltage regulator is shown in Fig. 4(a). The voltage regulator can be either DVR or STATCOM and are connected at node 6 and node 10 and the expanded figures are shown in Fig. 4(b) and Fig. 4(c) for DVR and

STATCOM respectively. Parameters considered for the simulation of the above-mentioned configuration are listed in Table 1.

**Table 1.** Parameters used for simulation of the considered system

Parameters	Values
Source/Grid Voltage	11 kV, 50 Hz
Feeder impedance	0.642 + j 0.083 Ω/km, Length of each section = 0.5 km
RES rating	0.75 MW for each unit of RES
CPL rating	1 MW for each CPL load
Constant Impedance load (CIL)	0.5 MVA each load, R = 193 Ω, L = 462 mH
DVR	0.5 MVA for each unit.
STATCOM	0.5 MVA for each unit.

Both the STATCOM and the DVR are assigned the same rating to evaluate their regulation proficiency. The effect of voltage control is reported for different levels of RES penetration: (i) RES penetration is high with perturbing loads ( $I_{RES} = 60$  A). (ii) RES penetration is low with perturbing loads ( $I_{RES} = 25$  A).

##### (i) High penetration of RES

In this case, high penetration of RES is considered, as each RES is generating maximum power as per its rating. In this scenario, the RES current  $I_{RES} = 60$  A (peak), resulting in each unit contributing 0.75 MW of power to the microgrid. The voltage profile is used to assess the responsiveness of DVR and STATCOM for voltage regulation in this scenario for several loading conditions. All the graphs, for each condition, show the voltage profile of the microgrid with considered loading conditions for:

- i. without any RES and voltage regulator connected to it.
- ii. with RES and without any voltage regulator connected to it.
- iii. with RES and DVR as the voltage regulator.
- iv. with RES and STATCOM as voltage regulators so that the regulation is accomplished by real current injection.
- v. with RES and STATCOM as voltage regulators so that the regulation is accomplished by reactive current injection.

**a. High penetration of RES and rated loading condition:**

The voltage profile of the microgrid with high penetration of RES at rated loading conditions, with each CIL drawing 0.5 MVA and each CPL drawing 1 MW power, is shown in Fig. 5(a). The voltage profile reveals that both the STATCOM and the DVR can regulate the voltage at their point of common coupling (PCC), i.e., at node 6 and node 10. DVR can regulate voltage with reactive power injection ( $V_{qDVR}$ ), whereas STATCOM ( $I_{dSTATCOM}$ ) can do the same with real power injection. Furthermore, Fig. 5(a) depicts the STATCOM's ( $I_{qSTATCOM}$ ) voltage profile while it is regulating through reactive power, yet the voltage does not reach the rated value even at the point of common coupling, but the profile is improved slightly.

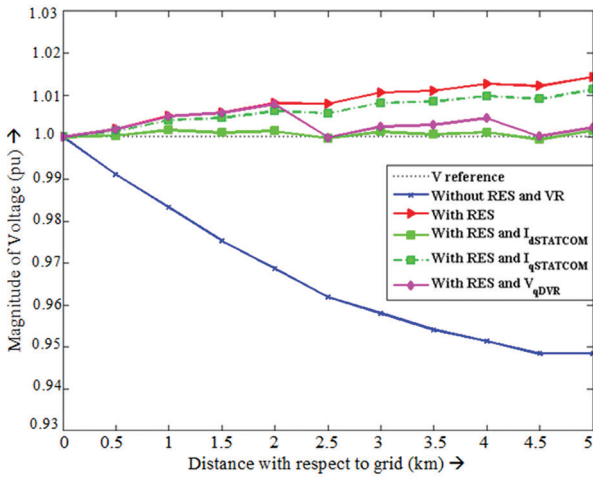


**Fig. 5.(a)** Voltage profile of microgrid with high RES penetration and rated loading condition

**b. High penetration of RES and light loading condition:**

The voltage profile of the microgrid with high penetration of RES and light loading conditions, i.e., 20% of the rated value, can be seen in Fig. 5(b). In this instance, the DVR improves the overall voltage profile of the microgrid by regulating the voltage at its two connecting points by absorbing a voltage that is a combination of both real and reactive power. However, since the range

required in this instance is relatively large, the STATCOM appears to be inadequate in regulating the voltage using either real or reactive current transactions.

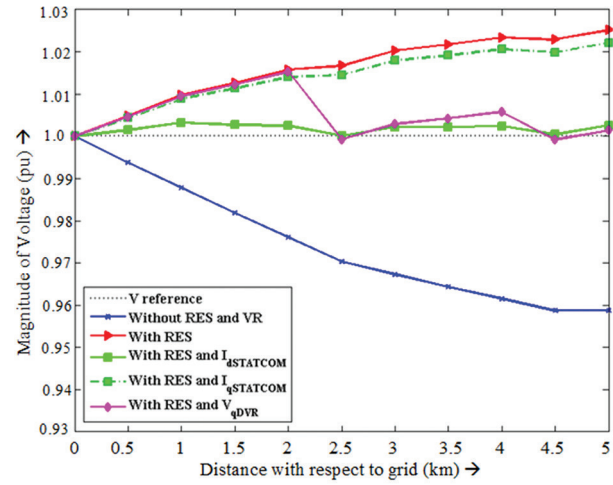


**Fig. 5.(b)** Voltage profile of microgrid with high RES penetration and light loading condition

**c. High penetration of RES and heavy loading conditions:**

Figure 5(c) depicts the voltage profile of a microgrid with high-RES penetration and heavy loading conditions of about 150% of the rated value. The voltage profile of the microgrid is enhanced with higher injection from RES because the loads are quite high.

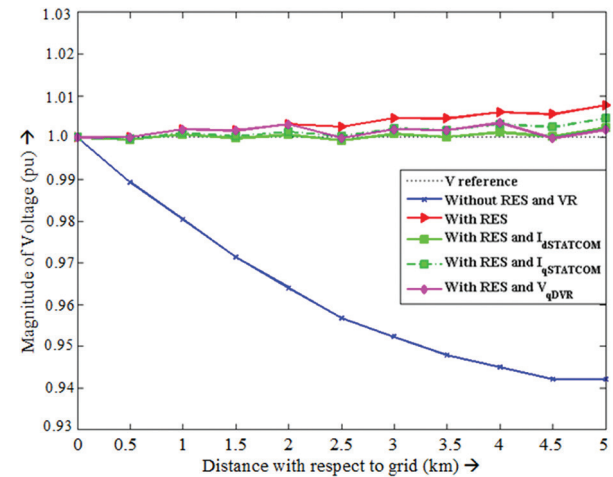


**Fig. 5.(c)** Voltage profile of microgrid with high RES penetration and heavy loading condition

As a result, both DVR and STATCOM improve the voltage profile even further.

**(ii) Low penetration of RES and normal loading condition:**

Injection from all the RES is reduced to 40% of the maximum value (given in the preceding scenario), with  $I_{RES} = 20$  A (rms), and each unit now supplies 0.30 MW of power to the microgrid.

**a. Low penetration of RES and normal loading condition:**

Figure 5(d) depicts the voltage profile of the microgrid under low RES penetration and rated load conditions. In this scenario, the DVR utilizes reactive voltage injection to regulate the voltage at its terminals, but the STATCOM employs real current injection.

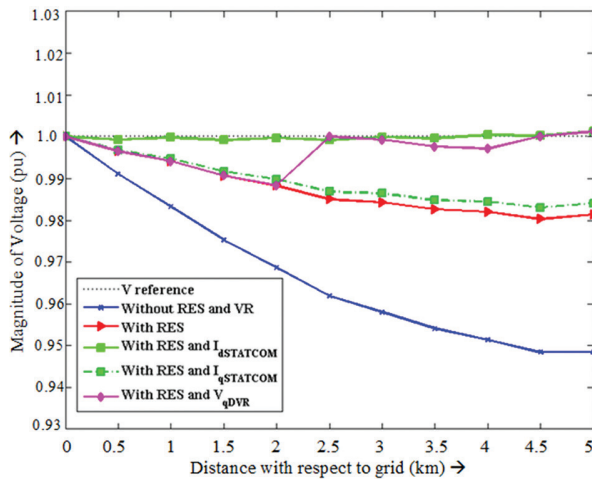


**Fig. 5.(d)** Voltage profile of microgrid with low RES penetration and rated loading condition

**b. Low penetration of RES and light loading condition:**

Figure 5(e) depicts the voltage profile of the microgrid at low RES penetration and light loading conditions, i.e. 20% of the rated value. As soon as the RES starts supplying power to the microgrid, the voltage profile improves. The voltage profile is further improved by both DVR and STATCOM.

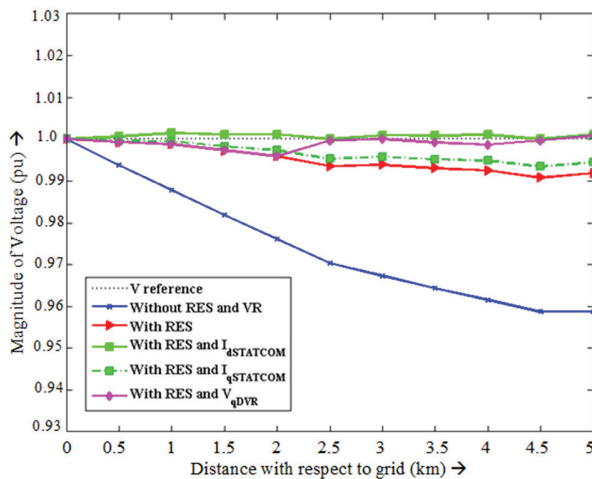


**Fig. 5.(e)** Voltage profile of microgrid with low RES penetration and light loading condition

**c. Low penetration of RES and heavy loading condition:**

Figure 5(f) depicts the voltage profile of the microgrid at low RES penetration and heavy loading conditions,

i.e. 150% of the rated value. Because the voltage variation is large in this scenario, the DVR requires both real and reactive power to perform, but it regulates the voltage, whereas the STATCOM is unable to do so even with both the real and reactive current injection.

**5. CONCLUSION**

The efficacy of DVR and STATCOM has been investigated and presented in this paper for improving the voltage profile of the 11-node radial microgrid with intermittent RES source in the MATLAB simulation environment. The PI controller and synchronous reference frame theory are used to control STATCOM and DVR. Voltage profiles obtained from the simulations demonstrate the comparison of the efficacy of DVR and STATCOM for voltage regulation in the microgrid. Under significant voltage variations, STATCOM can regulate the voltage only with real power support (through battery), while DVR allows voltage regulation with reactive power unless the voltage variations are extremely high. Utilization of STATCOM as a voltage regulator significantly increases the cost of the system as battery cost is also added to the system. In conclusion, the STATCOM is appropriate for voltage regulation if the range of compensation required is small, but as the range of compensation required widens, the DVR appears to be a superior solution.

**6. REFERENCES**

- [1] D. Ma, M. Liu, H. Zhang, R. Wang, X. Xie, "Accurate Power Sharing and Voltage Regulation for AC Microgrids: An Event-Triggered Coordinated Control Approach", IEEE Transactions on Cybernetics, 2021, pp. 1-11.
- [2] J. von Appen, M. Braun, T. Stetz, K. Diwold, D. Geibel, "Time in the Sun: The Challenge of High PV Penetration in the German Electric Grid", IEEE Power and Energy Magazine, Vol. 11, No. 2, 2013, pp. 55-64.
- [3] N. S. Jayalakshmi, P. B. Nempu, "Performance Enhancement of a Hybrid AC-DC Microgrid Operating with Alternative Energy Sources Using Supercapacitor", International Journal of Electrical and Computer Engineering Systems, Vol. 12 No. 2, 2021.
- [4] T. V. Krishna, M. K. Maharana, C. K. Panigrahi, "Integrated Design and Control of Renewable Energy Sources for Energy Management", Engineering, Technology & Applied Science Research, Vol. 10, No. 3, 2020, pp. 5857-5863.
- [5] V. Verma, R. Gour, "OLTC-DVR hybrid for voltage regulation and averting reverse power flow in the

micro-grid with intermittent renewable energy sources", Proceedings of the IEEE Industrial Electronics and Applications Conference, Kota Kinabalu, Malaysia, 2016, pp. 81-87.

- [6] Y. He, M. Wang, Z. Xu, "Enhanced Voltage Regulation of AC Microgrids with Electric Springs", Proceedings of the IEEE Applied Power Electronics Conference and Exposition, Anaheim, CA, USA, 17-21 March 2019, pp. 534-539.
- [7] A. Pimenta, P. B. C. Costa, G. M. Paraíso, S. F. Pinto, J. F. Silva, "Active Voltage Regulation Transformer for AC Microgrids", Proceedings of the IEEE 9<sup>th</sup> International Power Electronics and Motion Control Conference, Nanjing, China, 2021, pp. 2012-2017.
- [8] A. Ghosh, G. Ledwich, "Power Quality Enhancement Using Custom Power Devices", The Springer International Series in Engineering and Computer Science book series, 2002, pp 113-136.
- [9] R. Gour, V. Verma, "Voltage Regulation in a Radial Microgrid with High RES Penetration: Approach-Optimum DVR Control", Engineering, Technology & Applied Science Research, Vol. 12, No. 4, 2022, pp. 8796-8802.
- [10] H. M. A. Rashid, S. A. Jumaat, S. H. N. Yusof, S. A. Zulkifli, "Modeling the Grid Connected Solar PV (GCPV) System with D-STATCOM to Improve Stability System", Proceedings of the IEEE International Conference in Power Engineering Application, Shah Alam, Malaysia, 7-8 March 2022, pp. 1-6.
- [11] A. H. Soomro, A. S. Larik, M. A. Mahar, A. A. Sahito, A. M. Soomro, G. S. Kaloi, "Dynamic Voltage Restorer—A comprehensive review", Energy Reports, Vol. 7, 2021, pp. 6786-6805.
- [12] S. F. Al-Gahtani et al. "A New Technique Implemented in Synchronous Reference Frame for DVR Control Under Severe Sag and Swell Conditions", IEEE Access, Vol. 10, 2022, pp. 25565-25579.
- [13] L. E. Christian, L. M. Putranto, S. P. Hadi, "Design of Microgrid with Distribution Static Synchronous Compensator (STATCOM) for Regulating the Voltage Fluctuation", Proceedings of the IEEE 7<sup>th</sup> International Conference on Smart Energy Grid Engineering, Oshawa, ON, Canada, 12-14 August 2019, pp. 48-52.
- [14] A. P.N.Tahim, D. J. Pagano, M. L. Heldwein, E. Ponce, "Control of interconnected power electronic converters in dc distribution systems", Proceedings of the XI Brazilian Power Electronics Conference, 2011, pp. 269-274.
- [15] N. Ghanbari, S. Bhattacharya, "Constant Power Load Challenges in Droop Controlled DC Microgrids", Proceedings of the 45<sup>th</sup> Annual Conference of the IEEE Industrial Electronics Society, Lisbon, Portugal, 14-17 October 2019, pp. 3871-3876.
- [16] A. Engler, N. Sultanis, "Droop control in LV-grids", Proceedings of the International Conference on Future Power Systems, Amsterdam, Netherlands, 18 November 2005, pp. 1-6.